PROCEEDINGS OF SCIENCE

Tests and performance of multi-pixel Geiger mode APD's

Yuri Musienko[1,*]
Department of Physics, Northeastern University
360 Huntington Avenue, Boston, MA 02115, USA
E-mail: Iouri.Musienko@cern.ch

Stephen Reucroft
Department of Physics, Northeastern University
360 Huntington Avenue, Boston, MA 02115, USA
E-mail: Stephen.Reucroft@cern.ch

John Swain
Department of Physics, Northeastern University
360 Huntington Avenue, Boston, MA 02115, USA
E-mail: John.Swain@cern.ch

Systematic studies of recently developed multipixel Geiger mode APDs (G-APDs) from different manufacturers (CPTA, Dubna/Micron, Hamamatsu) are presented. The basic properties of G-APDs such as gain, photon detection efficiency, excess noise factor and noise, as well as their dependence on operating voltage and temperature have been measured. Spectral response was measured in the range 350–800 nm.

International workshop on new photon-detectors PD07
Kobe University, Kobe, Japan
27-29 June, 2007

[1] Speaker
[*] on leave from INR, Moscow, Russia

1. Introduction

During last decade, several groups announced the development of multi-pixel Geiger-mode APDs (G-APDs) [1,2,3]. The G-APD parameters (gain, PDE, excess noise factor, timing response) were reported to be similar or even superior to the parameters of PMTs. Recently, new G-APD structures have been developed. Improved performance of these photosensors (especially for detection of blue and UV photons) was reported by different investigators [4,5,6]. These results increased interest in G-APDs from HEP, astroparticle and medical communities

Correct evaluation of the G-APDs parameters and their influence on detector performance became very important. However measurement of these parameters (especially QE) is not an easy task due to the small sensitive area (typically 1 mm^2) and rather high dark count rates at room temperature. In the present work we present systematic studies of new devices from 3 different manufacturers using the methods proposed in paper [7].

2. G-APDs studied

For this paper we have studied the performance of 3 G-APDs which were developed by CPTA(Moscow)/Photonique(Geneva) [8], JINR(Dubna)/Mikron(Moscow) [9] and Hamamatsu Photonics (Japan) [10] (see Table1). The APDs from JINR and CPTA are both based on the n^+-p-p^+ structure. The third device (from Hamamatsu) has p^+-p- n^+ structure. All the G-APDs have 1 mm^2 sensitive area, which is subdivided into 556 (CPTA), 1024 (JINR) and 400 (Hamamatsu) separate pixels respectively. Each of these pixels is quenched by an individual resistor.

G-APDs	Producer's reference	Package	Protection	# of pixels	VB [V] (T=22 C)
CPTA/Photonique	SSPM_0701BG_PCB	PCB	No	556	30.7
Dubna/Mikron	pMP-3d-11	TO-18	Epoxy	1024	39.4
Hamamatsu	S10362-11-050C	Ceramic	Epoxy	400	68.8

Table 1. Basic properties of the G-APDs studied.

3. The dependences of the G-APDs gain and photon detection efficiency on the bias voltage

The definitions of basic G-APD parameters (such as photon detection efficiency (PDE), gain and excess noise factor (F)) as well as the measurement techniques used in this study are described in detail in our previous paper [7].

The gain and photon detection efficiency (PDE) of the G-APDs were measured using a green (515 nm) LED operated in pulsed mode. The signals from the G-APDs were amplified with a fast transimpedance amplifier (gain~30) and digitized with a LeCroy 2249W ADC

(gate=40 ns). The APDs were illuminated with small LED pulses via a 0.5 mm collimator. The number of photons in the LED pulse was measured using a calibrated XP2020 photomultiplier. This allowed the calculation of the G-APD gain and photon detection efficiency (PDE) as a function of voltage using the same measurement points. Fig. 1 shows a typical LED spectrum measured with CPTA G-APD at room temperature (T=22 C).

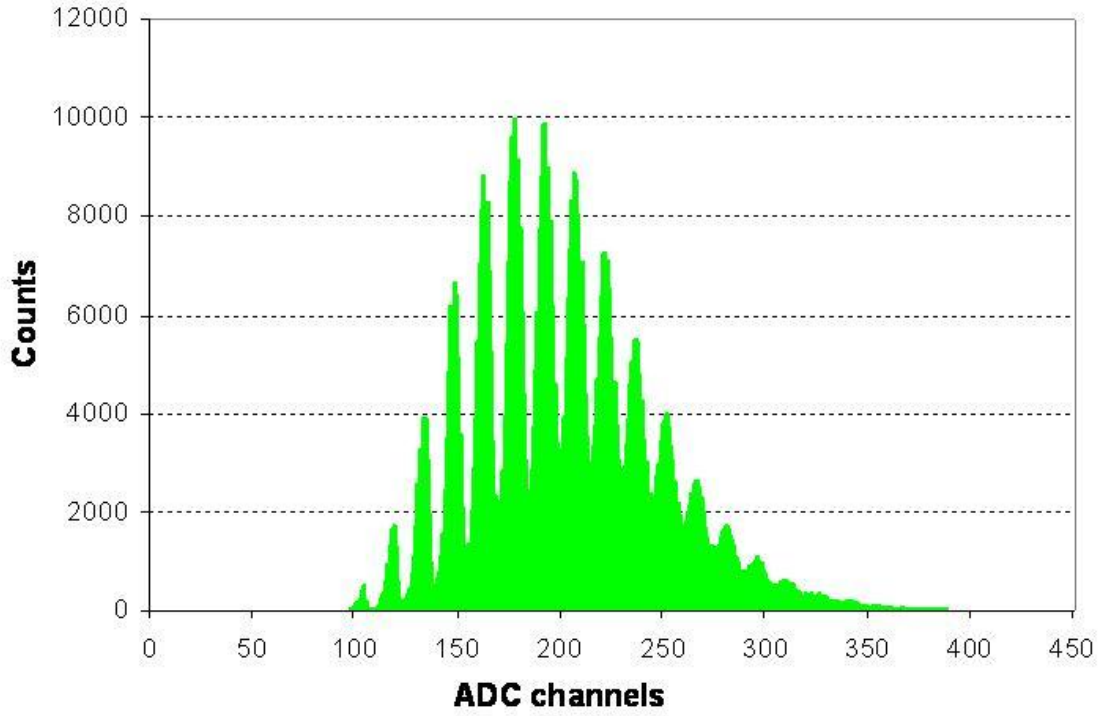

Figure 1: Low light LED amplitude spectrum measured with CPTA G-APD (U=39 V, T=22C).

The measured low light LED amplitude spectra (see, for example, Fig.1) can be compared with the Poisson distribution and the mean, N_{pe}, can be calculated using the well known property of this distribution:

$$N_{pe} = -ln(P(0)) \qquad (1)$$

Here $P(0)$ is the probability to observe the "pedestal" events. The average charge Q measured by the ADC in response to the LED pulse is related to the G-APD gain M_{APD} by:

$$Q = N_{pe} \times G_{amp} \times M_{APD} \qquad (2)$$

where G_{amp} is the gain of the amplifier. Equations (1) and (2) allow the calculation of the G-APD gain and photon detection efficiency (PDE) as a function of voltage using the same measurement points. The gain and PDE as a function of voltage of the CPTA, Dubna and Hamamatsu G-APDs (measured using 515 nm LED) are shown in Fig. 2 and Fig. 3.

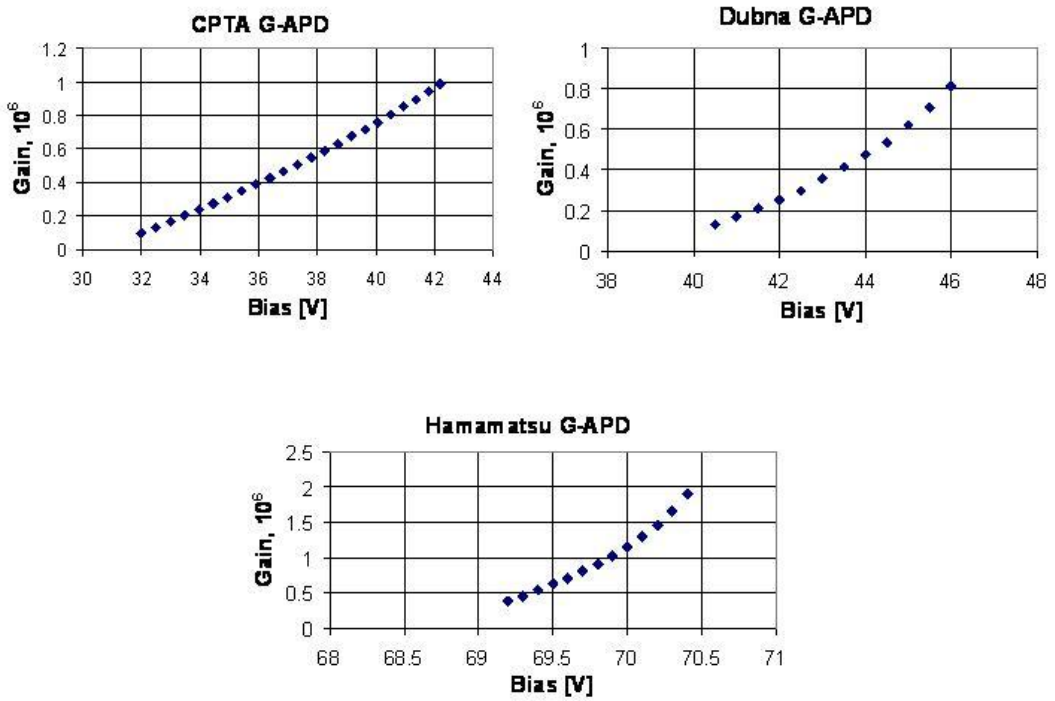

Figure 2: Gain as a function of voltage for the G-APDs measured at room temperature.

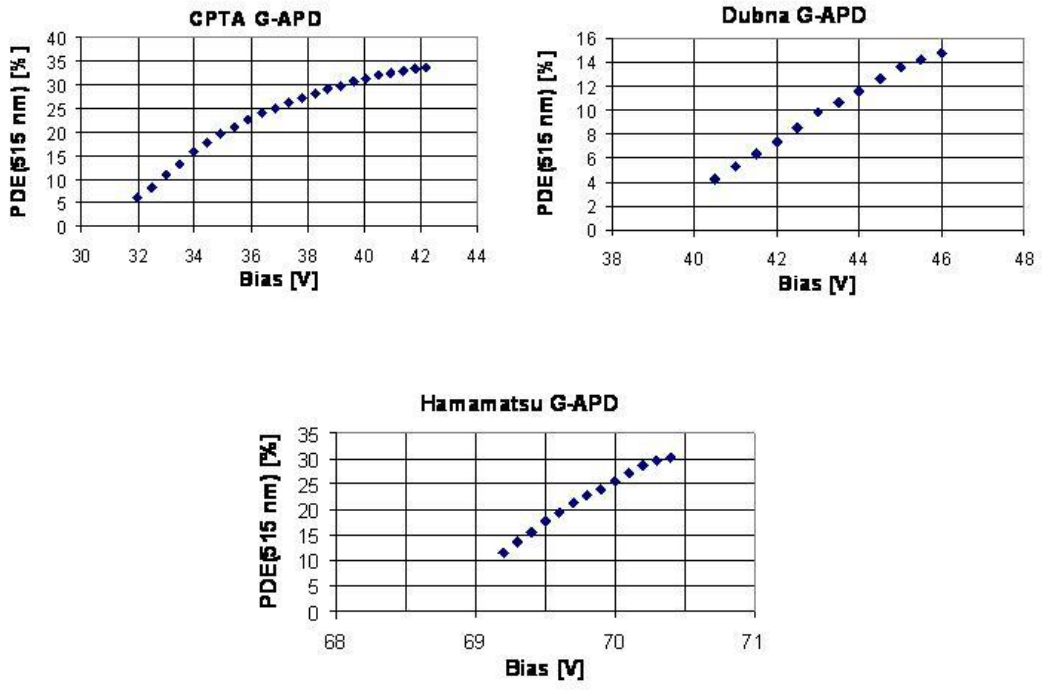

Figure 3: PDE as a function of voltage for the G-APDs measured at room temperature.

4. Multiplication noise of the G-APDs

Due to optical cross-talk between the pixels, the multiplication noise of the G-APD is not negligible as one would expect from the very small spread of the charge Q_1 for all the G-APD pixels (this spread is small due to small variations of the breakdown voltage over the 1 mm^2 APD area)[1]. This multiplication noise can be numerically expressed in a similar way as is usually done for PMTs and APDs operated below breakdown, in terms of an "excess noise factor", F. The G-APDs excess noise factor can be measured from the width of single electron spectra and calculated using:

$$F=1+\frac{\sigma_M^2}{M_{APD}^2} \qquad (3)$$

where M_{APD} is the G-APD gain and σ_M^2 is its variance. Another way (which gives the same result) is to compare the N_{pe} calculated from equation (1) and from N_w from the width of the measured spectra (number of measured photoelectrons should be small, or equivalently, *P(0)* should not be very low) . This method is easier to use:

$$F= N_{pe\,e}/\, N_w \qquad (4)$$

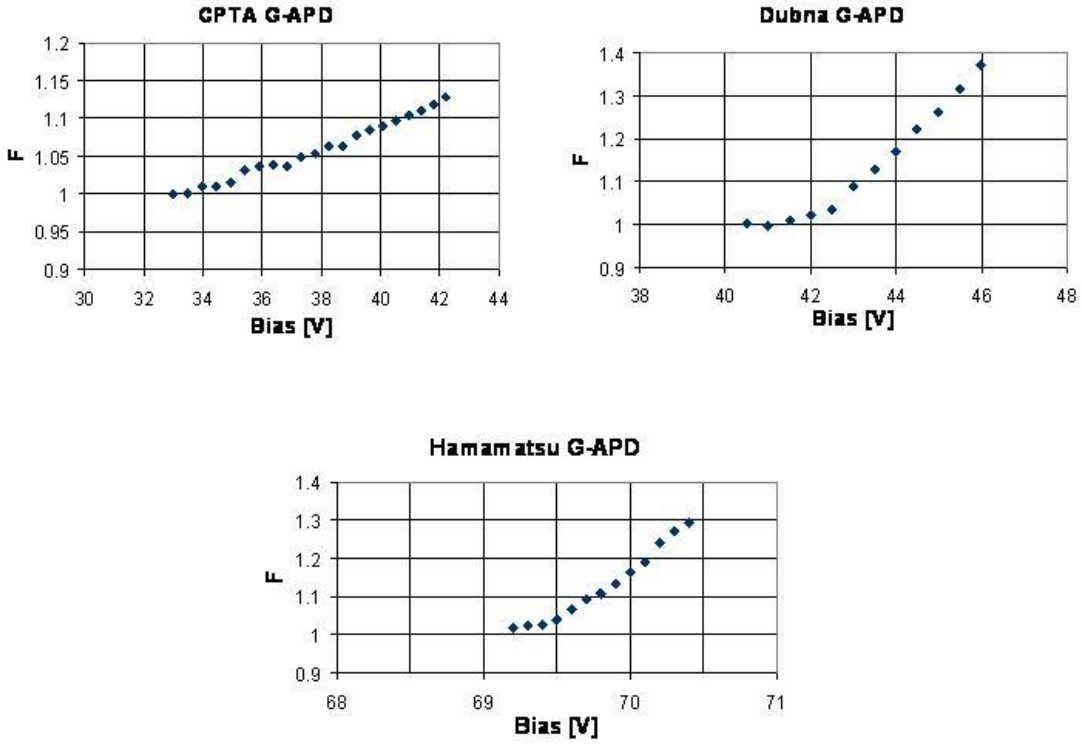

Figure 4: Excess noise factor as function of bias for CPTA, Dubna and Hamamatsu G-APDs

[1] "Afterpulsing" may also increase the G-APD's excess noise factor

Fig.4 shows F as function of bias for CPTA, Dubna and Hamamatsu G-APDs respectively. These results show that at high gains F is significantly different from unity for all 3 devices.

5. Dark count rate vs. bias voltage of the G-APDs

Dark count measurements were performed using a 300 MHz discriminator from Phillips Scientific (model 708). The discriminator threshold was set to the level corresponding to a 0.5 photoelectron G-APD signal. Fig. 5 shows the G-APDs dark count rates measured at room temperature.

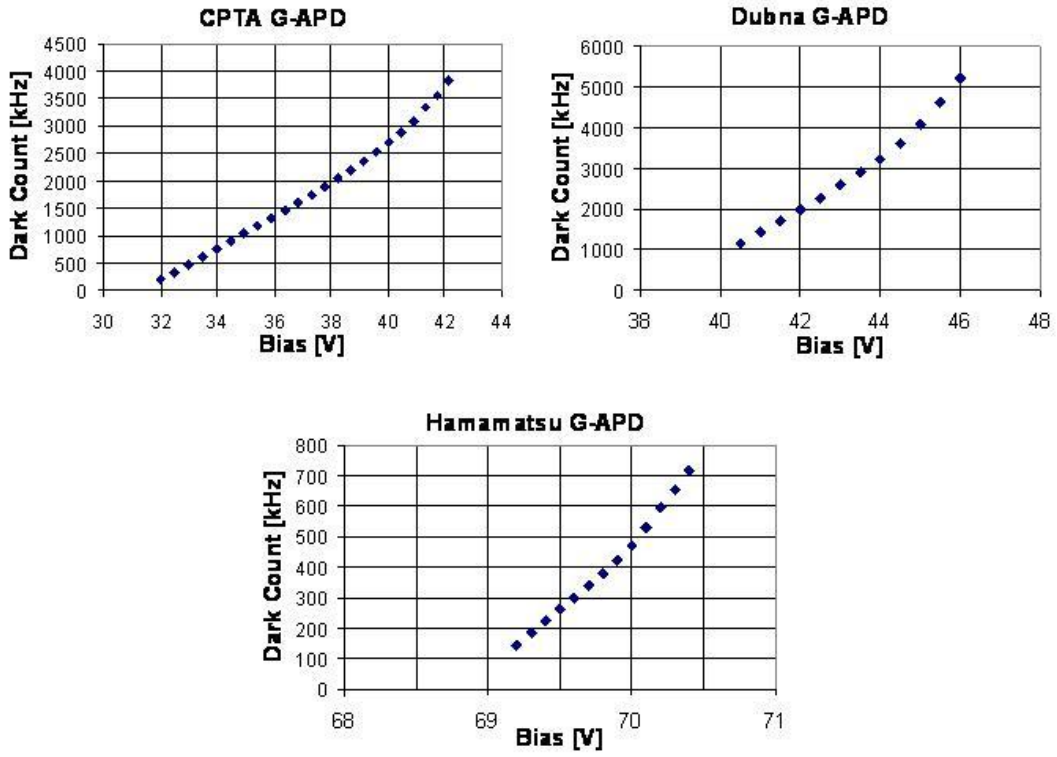

Figure 5: G-APDs dark count rates measured at room temperature (T=22 °C)

6. Voltage and temperature sensitivity of the signals from G-APDs

G-APD signal stability depends mainly on the stability of the applied bias and the temperature. To describe the dependence of the G-APD response on the bias and temperature one can introduce voltage coefficient as follows (see for example [8]):

$$k_V(V) = \frac{1}{A} \times \frac{dA}{dV} \times 100\% \qquad (5)$$

$$k_T(V) = \frac{1}{A} \times \frac{dA}{dT} \times 100\% \qquad (6)$$

Amplitudes of the signals were measured as functions of bias at 2 temperatures (T=22 °C and T=-25 °C). G-APD was placed inside a commercial freezer during these measurements. LED light was transmitted to the APD using quartz optical fiber. Fig. 6 shows the signal amplitudes as a function of the bias voltages for three G-APDs measured at 2 temperatures. From this figure one can see that the signal amplitudes increase for all 3 G-APDs when the temperature decreases. The amplitude curves have similar bias-voltage dependence at these temperatures. The values of breakdown voltages increase with increasing temperature. However the values of this increase are different for the different G-APDs. It was found that 1 °C temperature decrease causes the reduction of the breakdown voltages by 20 mV, 122 mV and 50 mV correspondingly for CPTA/Photonique, Dubna/Micron and Hamamatsu G-APDs. This is probably caused by the difference in the internal structure of these G-APDs.

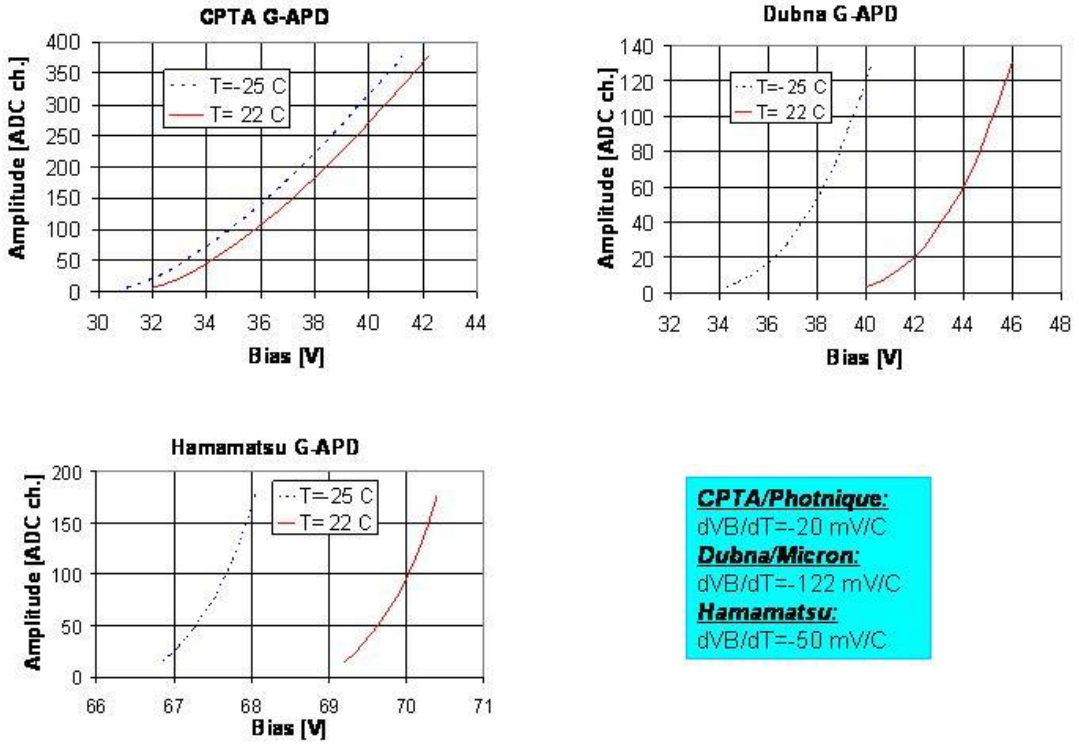

Figure 6: The signal amplitudes as a function of the bias voltages for three G-APDs measured at 2 temperatures

Voltage coefficients of the gain as functions of bias for three G-APDs have been calculated from the amplitude curves measured at room temperature. The results are shown in Fig. 7. Taking into account that amplitude curves have similar bias-voltage dependence at T= 22 °C and T=-25 °C equation 6 can be written as follows:

$$k_T(V) = \frac{1}{A} \times \frac{dA}{dT} \times 100\% = \frac{1}{A} \times \frac{dA}{dV} \times \frac{dV}{dT} \times 100\% = k_V \times \frac{dV}{dT} \qquad (7)$$

Equation 7 allows calculation of G-APD's temperature coefficients using corresponding values of voltage coefficients and values of *dVB/dT*. Temperature coefficients of 3 G-APDs in dependence on over-voltage (bias voltage minus breakdown voltage) are shown in Fig. 8.

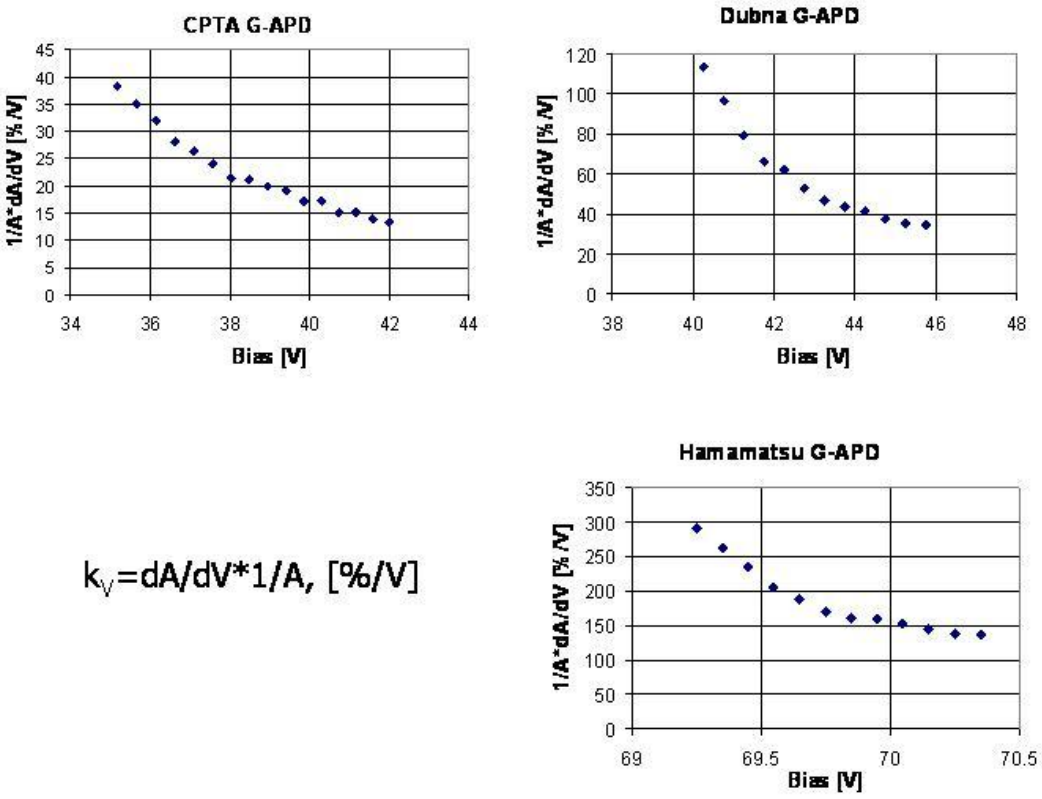

Figure 7: Voltage coefficients of 3 G-APDs in dependence on bias voltage (T=22 °C)

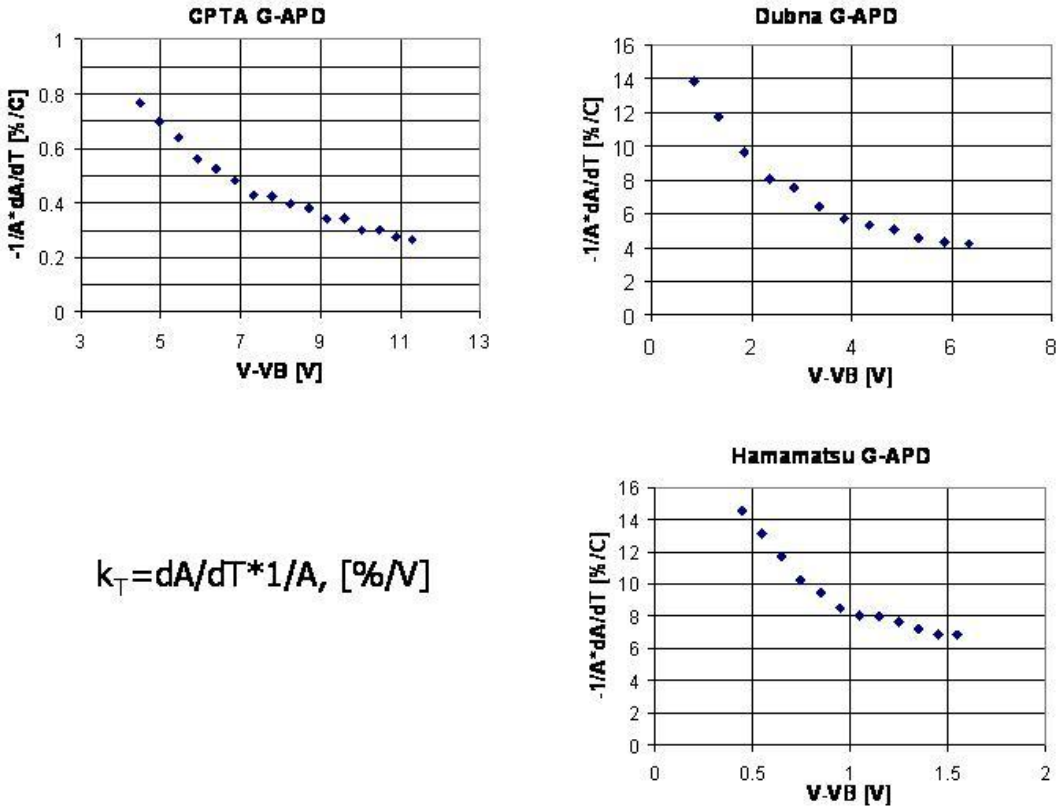

Figure 8: Temperature coefficients of 3 G-APDs as functions of over-voltage

7. Spectral response of the G-APDs

For the spectral response measurements an "Optometrics" SDMC1-03 spectrophotometer was used. We also used a calibrated PIN photodiode as a reference. Spectrophotometer light intensity was significantly reduced using gray filters to the level when the maximum current measured with the APD was only ~30% higher than its dark current. This was done to avoid the non-linearity effects caused by high pixel illumination. Photocurrent measured with the APD was compared with the photocurrent measured with the PIN photodiode. In addition the measurements with the LED pulsed light were used for absolute spectral response calibration (at least 2 different LED measurements were done for each APD). Fig. 9 shows the spectral response of the three G-APDs measured at room temperature for highest biases reachable by each G-APD (further increase of the bias voltage caused either high noise or instability of G-APD operation).

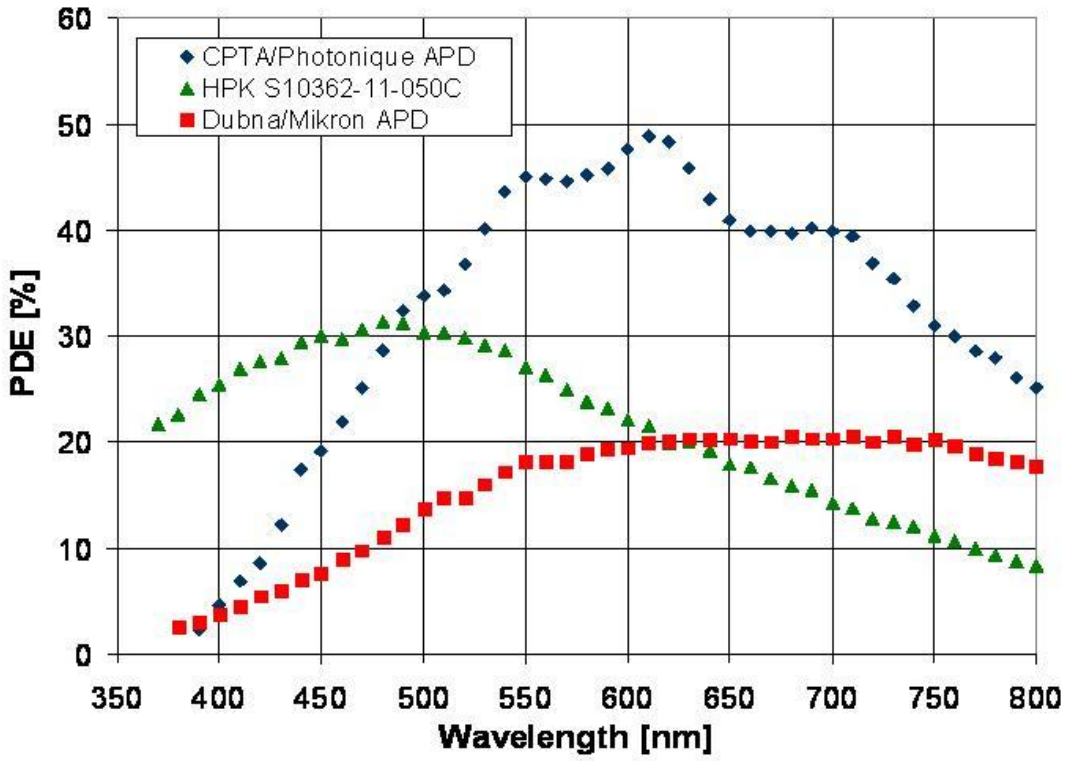

Figure 9: Photon detection efficiency as a function of the wavelength of light for 3 G-APDs measured at room temperature.

8. Summary

Recently developed G-APDs from 3 producers were studied in CERN APD Lab using technique developed by our group. Such G-APD parameters as photon detection efficiency, excess noise factor, dark count, gain, voltage coefficient of the gain, temperature coefficient of the gain and their dependence on the bias voltage were measured for 3 G-APDs at room temperature. Spectral responses were measured in the range 350–800 nm.

References

[1] G. Bondarenko, et al., *Nucl. Instr. and Meth.* A **442** (2000) 187.

[2] Z. Sadygov, et al., *Nucl. Instr. and Meth. A* **504** (2003) 301.

[3] P. Buzhan, et al., *Nucl. Instr. and Meth. A* **504** (2003) 48.

[4] I. Britvitch, et al., *Nucl. Instr. and Meth. A* **567** (2003) 276.

[5] E. Guschin, et al., *Nucl. Instr. and Meth. A* **567** (2003) 250.

[6] I. Britvitch, et al., *JINST.* 1 **P**08002.

[7] Y. Musienko, et al., *Nucl. Instr. and Meth. A* **567** (2003) 250.

[8] Photonique SA, Geneva , (http://www.photonique.ch).

[9] Dubna APD group, (http://sunhe.jinr.ru/struct/neeo/apd/).

[10] Hamamatsu Photonics, (http://www.hamamatsu.com)